Investigation on Grain Size Changes in Gamma Prime Precipitate on Varying Surface Location of IN738 Engine Turbine Blade

by

Muhammad A'izuddin Bin Nizam Shah
16439

Dissertation submitted in partial fulfilment of
the requirements for the
Bachelor of Engineering (Hons)
(Mechanical)

JANUARY 2016

Universiti Teknologi PETRONAS
32610 Bandar Seri Iskandar
Perak Darul Ridzuan

CERTIFICATION OF APPROVAL

Investigation on Grain Size Changes in Gamma Prime Precipitate on Varying Surface Location of IN738 Engine Turbine Blade

by

Muhammad A'izuddin Bin Nizam Shah
16439

A project dissertation submitted to the
Mechanical Engineering Programme
Universiti Teknologi PETRONAS
In partial fulfilment of the requirement for the
BACHELOR OF ENGINEERING (Hons)
(MECHANICAL)

Approved by,

……...
(Dr. Puteri Sri Melor Megat Yusoff)

UNIVERSITI TEKNOLOGI PETRONAS

SERI ISKANDAR, PERAK

January 2016

CERTIFICATION OF ORIGINALITY

This is to certify that I am responsible for the work submitted in this project, that the original work is my own except as specified in the references and acknowledgements, and that the original work contained herein have not been undertaken or done by unspecified sources or persons.

……..
(Muhammad A'izuddin Bin Nizam Shah)

ABSTRACT

A used nickel based gas turbine blade was received and it has been previously operated for more than 52000 hours and exposed to temperature approximately 720°C. The main purpose of this project is to investigate the grain size changes in gamma prime precipitate and to identify other different phases that occurred due to the high heat exposure. A few different locations of the turbine blade have undergone SEM to obtain the SEM images for grain size measurement and also EDX the to obtain the elemental analysis. It is found that the grain size of gamma prime precipitate varies throughout the surface of the turbine blade and there is a significant difference between the leading edge and the trailing edge. There are also different types of phases present at the microstructure of the blade due to extreme exposure to the turbine blade.

ACKNOWLEDGEMENT

First and foremost, I would like to thank all the people who has directly or indirectly involved in completing this project. A special appreciation to my supervisor, AP. Dr. Puteris Sri Melor Megat Yusoff for assisting and guided me throughout the whole process. A special thank you to Mr. Muhammad Aslam for helping me with the research and data analysis. Furthermore, I would extend my gratitude to the technologists that have helped me for the laboratory work, Mr. Mohd Danial Abdul Rani and Mr. Paris M Said. With their help, all the tasks and requirements that I have to complete will not be successful.

In addition, I would also like to acknowledge Univerisiti Teknologi PETRONAS (UTP) for having such a wonderful world-class facility and equipment that surely has contributed to the completion of the project. On top of that, the technologists that UTP possessed can be considered to be very knowledgeable and competent.

To all my friends and fellow course mates who have been supportive and helpful throughout the whole process. Last but not least to all my family who has been providing moral support in completing the project.

TABLE OF CONTENTS

LIST OF FIGURE

LIST OF TABLE

CHAPTER 1

INTRODUCTION

1.1 Background

Turbine blade is one of the most critical components in a gas turbine. From the high pressure gas and high temperature produced by the combustor, turbine blade functions to extract energy to produce mechanical work. Figure 1 shows the turbine blade located at the hot section side of a turbine, right after the combustion. Since the blades are prone to such environment, turbine blades are normally to be the limiting component in a gas turbine [1]. Turbine blades are usually made of superalloys. This is because superalloys are particularly well capable for these demanding applications. Even after being exposed for a long time at temperature above 650°C (1,200°F), they have the capability to retain most of their strength [2].

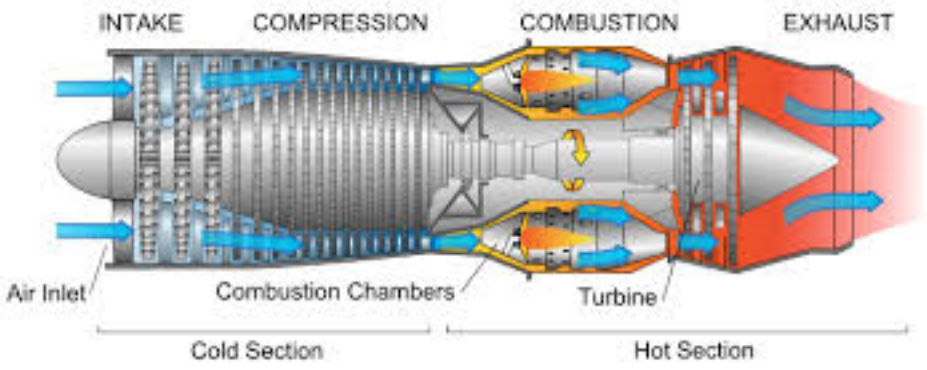

Figure 1: Gas turbine sections

After being exposed to high pressure and temperature, the grain size and microstructure of the blade will certainly be affected. During service, the blades experience the effect of high stresses and temperatures, which unavoidably causing

various microstructural changes. The changes in the microstructure can lead to degradation of mechanical properties such as tensile strength, creep resistance and others [3].

Throughout the years, there has been a lot of research regarding gas turbine blade. Titanium alloys, steel and Nickel are some of the materials that have been used to fabricate gas turbine blades. Each material has different grain size and microstructure thus having different outcome and cause of failure. This is because microstructure plays a significant role in influencing the performance and lifespan of the gas turbine blade [4-5]. Materials properties such as ductility, strength, toughness, density are also influenced by the microstructure.

1.2 Problem Statement

Turbine blade is a very critical component in a gas turbine. After being exposed to extreme temperature and pressure, different mechanical properties of the blade will be affected. The service life or lifespan of the turbine blade to function also is affected due to such exposure. Once the turbine blade is damaged, the repairing and replacing of a new turbine blade will be costly and will also affect the productivity. At different location of the turbine blade, it will have different grain size particles and microstructures. This is mainly because of the difference of high temperature that the blades were being exposed to. Therefore a comprehensive study on the shape and size of the grains differences will be studied to determine the effect, the changes and the phases that occur from the exposure of such environment.

1.3 Objectives

To measure the grain size of the Gamma Prime precipitates of the used turbine blade

The study is focused on measuring the grain size of γ′ precipitates quantitatively and to relate the size to the different surface locations of the turbine blade. Other major phase presents in the Nickel-based superalloys such as carbides are also to be studied in this project.

1.4 Scope of Study

From the Scanning Electron Microscope (SEM) images obtained from the previous study, the grain size is measured by using ImageJ software. The software in an open source software that can be downloaded in the Internet. Mean size of the grains was measured at 14 different surface locations of the blade.

Energy-dispersive X-ray Spectroscopy (EDX) analysis was carried out to determine the composition of each phase but only two samples were taken, one from the edge of the turbine and the other one at the center of the blade. The elemental compositions are compared at different spots of the two respective samples.

CHAPTER 2

LITERATURE REVIEW

2.1 Material of The Turbine Blade

Nickel-based superalloys are the most common materials for manufacturing of turbine blade. These alloys have the ability to resist very forceful environment found within turbine engine's hot gas path which are high temperature and high stress. Nickel is considered as a most suitable basis for alloying. This is because it has the almost-full third electron shell, a high capacity for forming stable alloys without instability phase. Considered to be protective and stable, both of the metallic elements movement in the outward direction and aggressive atmospheric elements such as sulphur, oxygen and nitrogen in an inward direction are restricted. On top of that, by adding aluminium, Nickel will form Al_2O_3 surface layers. These layers are highly oxidation-resistant at very high temperatures [6]. Table 1 shows types of nickel materials used for turbine blades.

Table 1: Nominal cast of superalloys {7]

	Nominal composition, %												
Alloy designation	**C**	**Ni**	**Cr**	**Co**	**Mo**	**Fe**	**Al**	**B**	**Ti**	**Ta**	**W**	**Zr**	**Other**
Nickel-base													
B-1900	0.1	64	8	10	6	. . .	6	0.015	1	4(a)	. . .	0.10	. . .
CMSX-2	. . .	66.2	8	4.6	0.6	. . .	56	. . .	1	6	8	6	. . .
CMSX-4	. . .	bal	6.5	9	0.6	. . .	5.6	. . .	1.0	6.5	6	. . .	
CMSX-6	. . .	bal	10	5	3	. . .	4.8	. . .	4.7	2	. . .	. . .	
CMSX-10	. . .	bal	1.8–4.0	1.5–9.0	0.25–2.0	. . .	5.0–7.0	. . .	0.1–1.2	7.0–10.0	3.5–7.5	. . .	
Hastelloy X	0.1	50	21	1	9	18	. . .	. . .	. . .	. . .	1	. . .	. . .
Inconel 100	0.18	60.5	10	15	3	. . .	5.5	0.01	5	. . .	. . .	0.06	1 V
Inconel 713C	0.12	74	12.5	. . .	4.2	. . .	6	0.012	0.8	1.75	. . .	0.1	0.9 Nb
Inconel 713LC	0.05	75	12	. . .	4.5	. . .	6	0.01	0.6	4	. . .	0.1	. . .
Inconel 738	0.17	61.5	16	8.5	1.75	. . .	3.4	0.01	3.4	. . .	2.6	0.1	2 Nb
Inconel 792	0.2	60	13	9	2.0	. . .	3.2	0.02	4.2	. . .	4	0.1	2 Nb
Inconel 718	0.04	53	19	. . .	3	18	0.5	. . .	0.9	. . .	. . .	. . .	0.1 Cu, 5 Nb
X-750	0.04	73	15	. . .	. . .	7	0.7	. . .	2.5	. . .	. . .	. . .	0.25 Cu, 0.9 Nb
M-252	0.15	56	20	10	10	. . .	1	0.005	2.6	. . .	. . .	. . .	. . .
MAR-M 200	0.15	59	9	10	. . .	1	5	0.015	2	. . .	12.5	0.05	1 Nb(b)
MAR-M 246	0.15	60	9	10	2.5	. . .	5.5	0.015	1.5	1.5	10	0.05	. . .
MAR-M 247	0.15	59	8.25	10	0.7	0.5	5.5	0.015	1	3	10	0.05	1.5 Hf
PWA 1480	. . .	bal	10	5.0	. . .	. . .	5.0	. . .	1.5	12	4.0	. . .	. . .
PWA 1484	. . .	bal	5	10	2	. . .	5.6	. . .	. . .	9	6	. . .	
Rene 41	0.09	55	19	11.0	10.0	. . .	1.5	0.01	3.1	. . .	. . .	. . .	. . .
Rene 77	0.07	58	15	15	4.2	. . .	4.3	0.015	3.3	. . .	. . .	0.04	. . .
Rene 80	0.17	60	14	9.5	4	. . .	3	0.015	5	. . .	4	0.03	. . .
Rene 80 Hf	0.08	60	14	9.5	4	. . .	3	0.015	4.8	. . .	4	0.02	0.75 Hf
Rene 100	0.18	61	9.5	15	3	. . .	5.5	0.015	4.2	. . .	. . .	0.06	1 V

As for this project, the material of the blade is IN738. IN738 is a material that is Nickel-based superalloy, which is strengthened by gamma prime precipitation. Furthermore, this type of material is widely used to fabricate turbine blades in gas turbine engine at hot sections part. Besides that, it has such exceptional strength properties at extreme exposure of high temperature and stress.and also great hot corrosion resistance [8]. The weight precentage of of IN738 compositions is shown at Table 2.

Table 2: Chemical composition in weight percentage (%) of IN738 [9]

Ni	Cr	Co	Ti	Al	W	Mo	Ta	Nb	C	Fe	B	Zr
Bal.	15.84	8.5	3.47	3.46	2.48	1.88	1.69	0.92	0.11	0.07	0.12	0.04

Usually, this type of cast Nickel-based superalloy is used as the blade material in the first row of the high pressure stage of a gas turbine. There are different type of phases present in this particular alloy namely FCC γ matrix, bimodal primary and secondary γ' precipitates, γ- γ eutectic, carbides and a small amount of damaging phases such as σ, δ, η and Laves which fall under the Topologically Close-Packed Phases [9].

2.2 Microstructure Influence

There are 4 major microstructural phases present in nickel-based superalloys [2]. Each phase has different characteristics and properties. The phases are :

i) Gamma (γ)

ii) Gamma Prime (γ′)

iii) Carbides

iv) Topologically Close-Packed Phases (TCP)

Gamma (γ) is a face-centered cubic (FCC) nickel-based. γ phase is considered as a continuous matrix. Co, Cr, Mo, and W , which usually have in high percentage, are some of the examples of solid-solution elements present at this specific phase [2].

Gamma Prime (γ′) or $Ni_3(Al,Ti)$ is the primary strengthening phase in a nickel-based superalloy. With an ordered LI_2 (FCC) crystal structure, it is considered to be a comprehensive precipitating phase. Remarkably, with increasing the temperature to around 650^{o}C, the flow stress of the γ′ is also increased. Besides that, γ′ is quite ductile. Therefore without lowering the fracture toughness of the alloy, γ′ imparts strength to the matrix. The major constituents are titanium and aluminium. They are added with proportions to precipitate a high volume fraction in the matrix. The volume fraction of the γ′ precipitate is around 70% for some of the modern alloys [2]. Different shapes and sizes of the γ' precipitate have been observed such as cubes, spheres, plates, rafts and many more [10]. The distribution of γ′ phase, the volume fraction and size of the cell are important to control different mechanical properties such as creep [9-10].

Nickel-based superalloys are age-hardenable by a fine dispersion of γ′ particles. The mechanical properties of alloy are strongly dependent upon the size and distribution of the γ′ precipitates. During the initial heat treatment and subsequent service, it is critical to forecast the coarsening kinetics of this precipitate. This is because the γ′ particles can coarsen during that particular period [11].

As the particles coarsen, γ′ precipitates shape will generally change from cuboid to sphere. This is because of the lattice mismatch between the γ matrix and γ′ precipitate. Further coarsening of the of γ′ precipitates will make the particles flattter and thus cause the cuboidal shape to elongate. This is called the split phenomenon of γ′ precipitate particles [12].

Carbides are formed when refractory and reactive elements such as Tantalum, Titaniun or Hafinum are combined with carbon. Carbides will begin to decompose and form lower carbide for example M_6C and $M_{23}C_6$ during heat treatment and service. They also will start to form along grain boundaries. Most of the common carbides are FCC crystal structure. Carbides can be both advatageous or harmful to the superalloy properties depending on the variation of the results. Most of the time, it is believed with the presence of grain boundaries in a superalloys, they are beneficial and helpful since it will increase rupture strength at high temperature [2].

The microstructure of an alloy will undergo overaging due to prolong exposure to high stress and thermal environment. Some examples on the impact of such exposure are primary MC carbide degeneration, formation of continuous secondary $M_{23}C_6$ carbide films on the grain boundaries, σ -phase formation and γ′ phase coarsening and coalescence. All of these will have a harmful effect on creep-resistant properties[3].

As for **Topologically Close-Packed Phases (TCP),** they are considered to be unwanted and undesirable phase that occurred during service and heat treatment. At this phase as well, the structure of the cell will have layers of close-packed atoms separated comparatively by large interatomic distances. This plate-like structure will give mechanical properties such as creep rupture and ductility negative impact. TCPs are considered to be detrimemtal due to their brittle nature that can initiates cracks and also can reduce creep strength when TCPs are tied up with γ and γ’ strengthening element in a non favorable form [2].

CHAPTER 3

METHODOLOGY

3.1 Research Methodology/ Analysis

This project mainly focused on the metallography analysis. It consists of the study and investigation of the physical component and structure of the metal. The analysis is generally using microscopy.

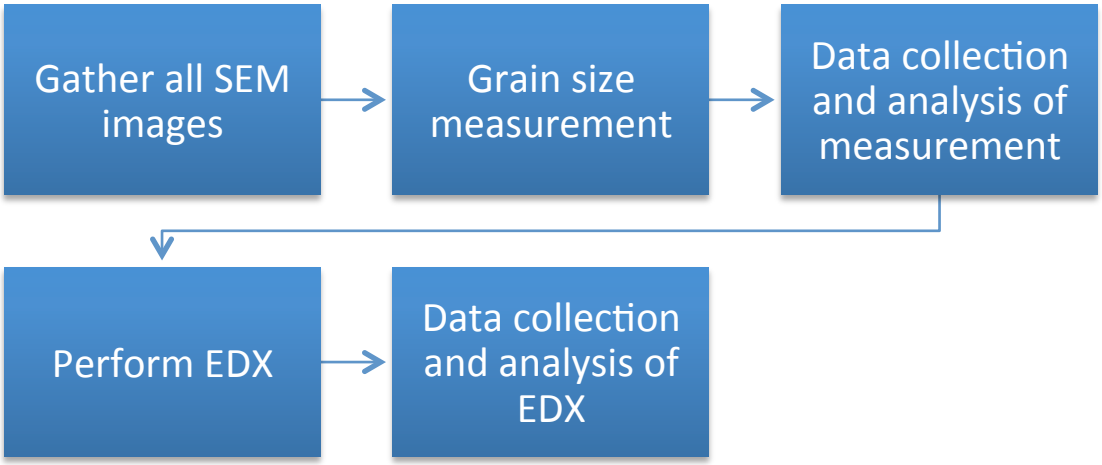

Figure 2: Summary of project methodology

In this project, all of the procedures will be implemented accordingly. The grain size of γ' precipitates are measured quantitatively. Besides that, EDX analysis was carried out at two locations, with four different spots are being focused on at both locations. Each of the spot is expected to represent different phase of the IN738 Nickel-based superalloys.

3.2 Material Preparation

Previously, a study has been conducted on this project. Therefore, the sample materials have already been prepared and the samples have undergone Scanning Electron Microscopy (SEM) analysis. 14 different locations have been cut and sectioned from the turbine blade.

Here are the steps that were taken in preparing the samples. The sample was prepared and sectioned by using electric discharge machine. Firstly, from the original turbine blade, it was cut into two halves. Figure 3 shows the first half of the blade, which is the suction side while Figure 4 shows the pressure surface side of the blade. For the small samples sectioning, two samples from both type of surfaces that are near to the leading edge were cut making a total of four samples, namely A1, B1, A2 and B2. Same approach was used to get another four samples that are close to the trailing edge for both of the blade's surfaces, which are C1, D1, C2 and D2. Another four samples were taken at the center of the blade for both suction and pressure surface sides of the blade, namely E1, E2, F1 and F2. The last two samples which are A3 and B3, shown in Figure 5, were cut at the leading edge of the blade.

Once the sectioning and cutting process was done, the samples were mounted by using Buehler Simplimet 1000 Automatic Mounting Presses machine. The samples were then proceed to the grinding and polishing process until mirror image is formed on the surface of the samples. These processes were done by using Buehler Metaserv 2000 machine manually. For grinding, the samples were ground using Grit 240 to 1200 silicon carbide paper. For polishing, 6μm alumina followed by 1μm alumina was used with distilled water as suspension solution on low napped polishing cloth. As for etching process, for two to three minutes, the sample was immersed and swabbed by Kalling's agent consists of 40ml of Ethanol, 40ml of HCL and 2g of $CuCL_2$ was used to reveal the microstructure.

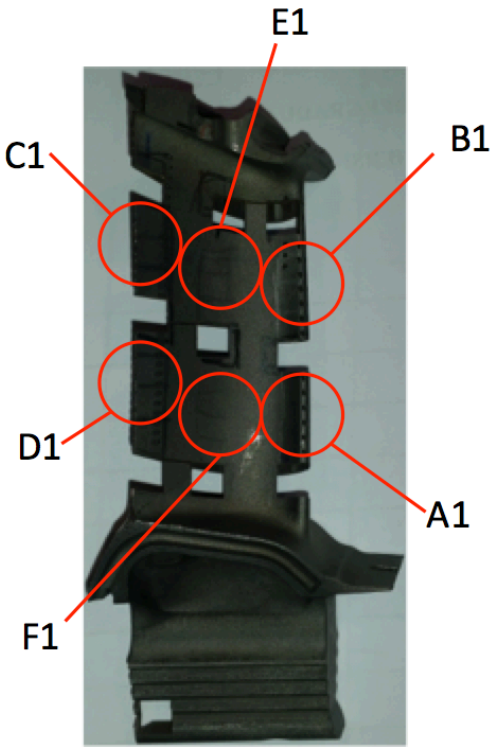

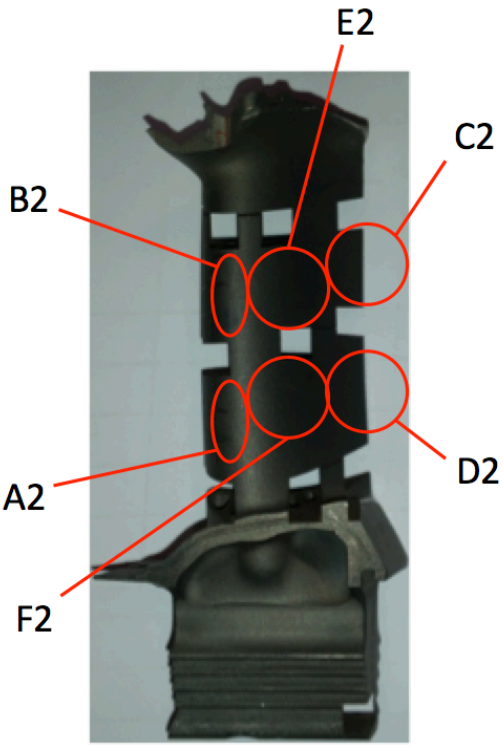

Figure 3: Suction surface side of the blade Figure 4: Pressure surface side of the blade

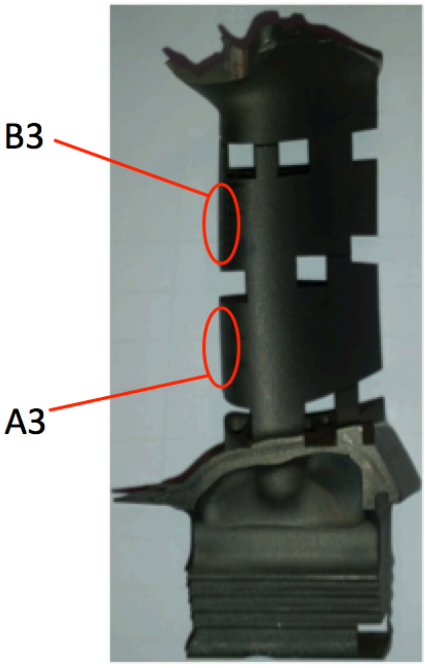

Figure 5: Samples at the leading edge at the surface section side

After that, SEM analysis was carried out to examine the Gamma Prime Precipitate and the microstructure of each sample. From the SEM images as well, other phase like carbide are also analysed and studied The machine used for the previous study analysis was Zeiss SUPRAA55VP . While for the current study, for EDX analysis, Phenom ProX was used to determine the elemental composition.

Since it is a continuation from the previous study, EDX analysis that has to be performed required the samples to be prepared again. Therefore, the mounted sample of the turbine has to be grinded, polished and etched again. Therefore, two samples were taken for the preparation process. The first sample was A3, which is located at the leading edge of the turbine blade. While the other sample chosen was at location F1, which is located at the center of the turbine blade. From this analysis, the microstructure's elemental composition can be obtained thus the phases that occurred on the blade can be determined.

For the EDX analysis, two samples that are believe to show different phases of the turbine blade are chosen. 4 spots from each image sample is pointed so that the elemental composition of the phase can be obtained. Therefore, the phases of the microstructure can be determined.

3.3 Measuring Technique

To measure the Gamma Prime precipitate quantitatively, an open source software is used. The software is called ImageJ and it can be downloaded for free in the Internet. Figure 6 shows the technique used to measure the grain size. The longest length of the grain was measured. After measuring all the grains in the image, the measurements are tabulated.

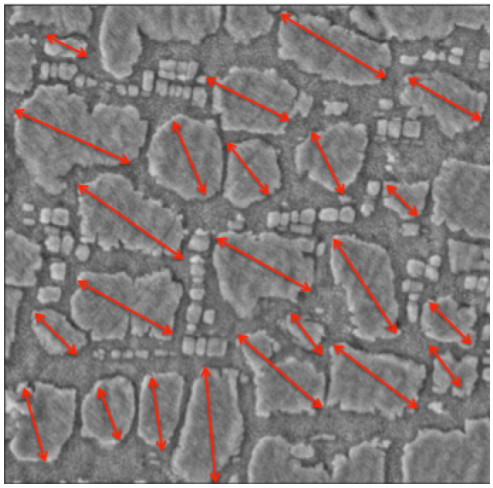

Figure 6: The technique used to measure the size of the grains

For consistency, only a section of the whole image was cropped and selected for the measuring process. At each location, a SEM image of 5.0K X magnification was chosen. This procedure was carried out to all the other locations of the turbine blade.

3.4 Gantt Chart and Key Milestones

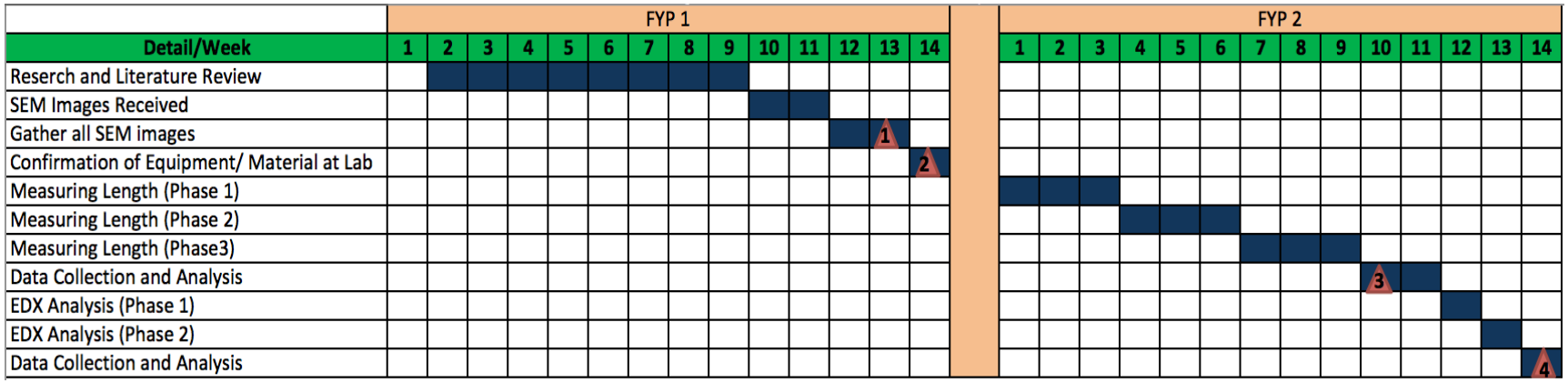

Figure 7: Gantt Chart and Key Milestone

CHAPTER 4

RESULTS AND DISCUSSION

4.1 Microstructural Observation

One of the results obtained by using SEM as shown in Figure 6 was analysed and studied. The location of the SEM image shown is at location D1. Obviously, different size and shape of the gamma prime precipitates are observed from the image.

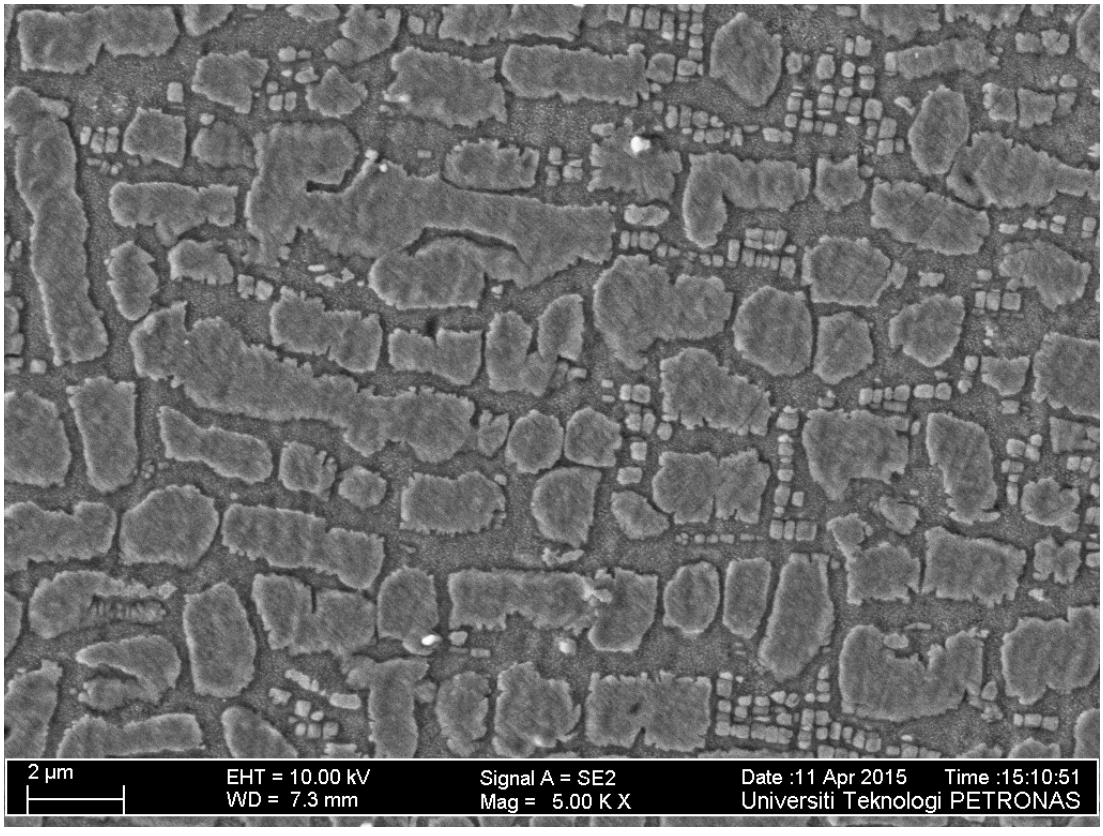

Figure 6: Different size of Gamma Prime Precipitates

Most of the gamma prime precipitate has a cubical or spheroidal shape. There are also elongated gamma prime precipitate observed from the microstructure image. It is believed that these elongated precipitates are the effect of coarsening at the precipitate. This was due to extreme exposure to the surface of the turbine blade during service.

From the SEM images as well, other phase like carbide are also analysed and studied. As shown in Figure 8, which is location A3 of the turbine blade, aligned carbide can be seen clearly. The distrubution of the gamma prime precipitates is bimodal where the primary and secondary gamma prime precipitates are mixed around.

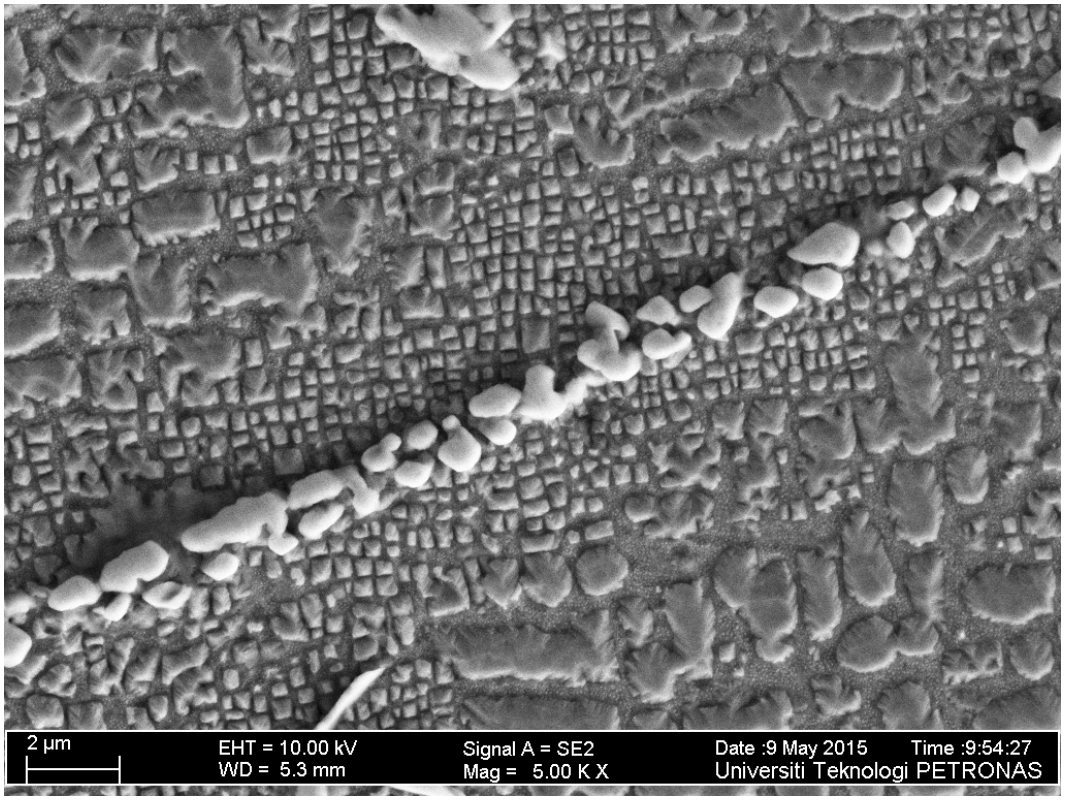

Figure 7: Presence of aligned carbides

Throughout the whole turbine blade, at all locations, the presence of aligned carbides were observed. It proves that the blade has exposed to the very high temperature thus causes the propagation of the carbides.

4.2 Mean Size of Gamma Prime Precipitate

From the size measurement by using ImageJ software, the results obtained proves that the mean length of the grain size varies at different surface locations of the engine turbine blade as shown in Table 3. This is due to the different exposure at different location at the turbine blade.

Table 3: The mean size of Gamma Prime Precipitate at all locations

Location	A1	A2	A3	B1	B2	B3	C1
Length(um)	1.892	2.364	1.608	1.637	0.792	2.115	2.304
Location	C2	D1	D2	E1	E2	F1	F2
Length(um)	3.002	1.846	0.683	2.048	1.531	2.782	1.649

From Table 3 as well, it shows that the maximum grain size is located at the trailing edge of the blade which is at location C2 with the value of 3.002µm. For the leading edge, the minimum grain size length is at location A3 with the value of 1.608µm. Comparing the mean grain size at the leading edge and trailing edge, it can be concluded that the mean length of both edges have a notable differences. Leading edge has a mean length of 1.735µm while the mean length of trailing edge is 1.959µm. This shows that the leading edge gas a lower mean size compared to the trailing edge. As for the difference between the two surface sides and the blade, pressure surface side has a lower average grain size compared to the suction surface side. Pressure surface side has an average length of 1.670µm while suction surface side has recorded a value of 2.084µm.

This is due impingement cooling where cooling air is injected to the blade. Since the temperature exposed to the blade is so high, cooling process is introduced to the blade. Cooling air enters from the leading edge. Through the small holes that is designed at the blade, cool air that was received from the compressed air from the compressor will give a cooling effect to the blade. Thus, the hot air will not massively affect the blade [13].

Obviously, heat travels from hot to cold. Therefore, when the heat was exposed at the leading edge, heat will travel to the colder part of the blade, which is the trailing edge. With that happening at both edges of the blade, it does mean that the trailing edge suffered more constant hot condition compared to the leading edge. This is because there

is always cool air injected to the leading edge although it was exposed to the hot air first. This will make the grain size at the trailing edge more coarsen thus producing a longer length of gamma prime precipitate. Same concept also occurs at both surface sides of the blade

The histogram as shown in Figure 10 is the tabulation of data for the frequency against mean length range. It indicates that the grain size varies at different surface location of the blade with the mean length range of 1.600 – 2.099 μm shows the highest frequency with 6. The majority suface blade's location is near to the leading edge.

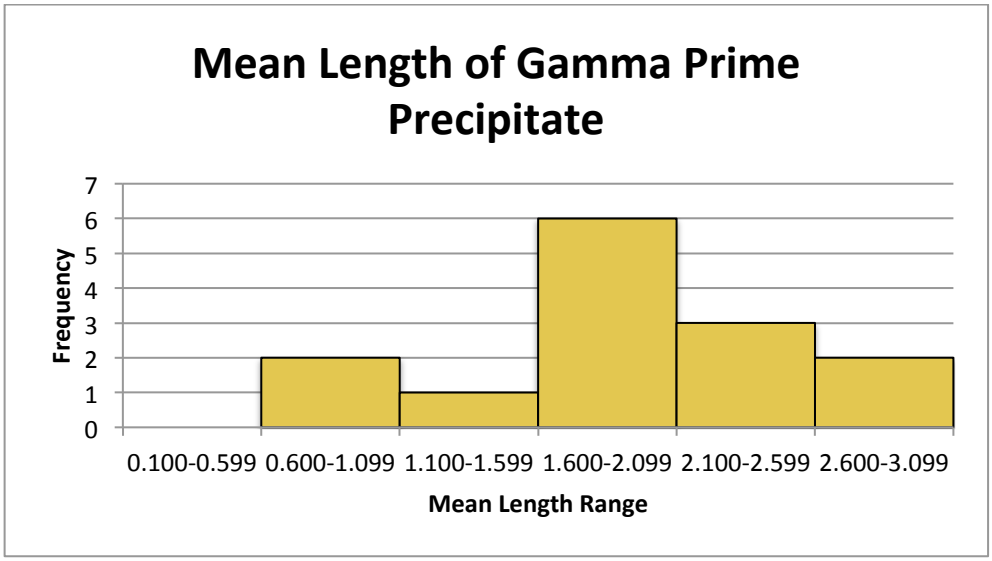

Figure 10: Histogram for mean length of Gamma Prime Precipitate

4.3 EDX Analysis

Energy-dispersive X-ray Spectroscopy (EDX) is carried out to obtain the elemental analysis of the turbine blade. As mentioned in the methodology part, two samples were chosen for this analysis, namely location A3 and F1.

4.3.1 EDX at Location A3

Figure 11 show the image obtained from the analysis at location A3. Four different spots were chosen for the EDX analysis. Each spot would represent different phases that occurred in the microstructure.

Figure 11: 4 spots taken at location A3

Spot 1 is believed to be a Tantalum-based carbide. This is because there is the presence of Carbon. Tantalum has recorded the highest concentration at this spot with 45.1%. Besides that, the concentration of Nickel is very low with 2.7% only. This clearly proves that the white aligned structure is carbide. Spectrum in Figure 12 shows that Tantalum is at the highest peak. Table 4 shows the rest of the elements present at spot 1.

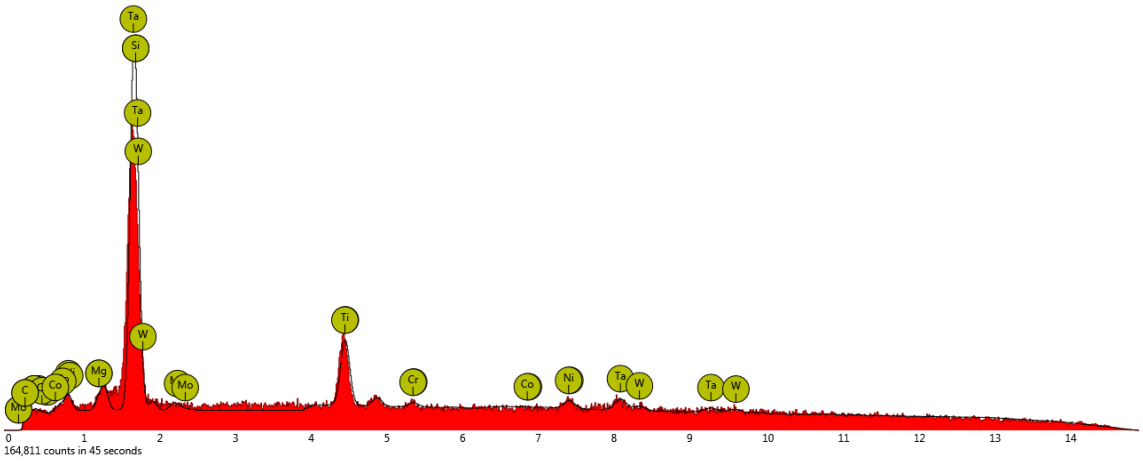

Figure 12: Elemental composition at spot 1, location A3

Table 4: Elements detected in spot 1, location A3

Atomic Number	Element Symbol	Element Name	Concentration (%)	Certainty
73	Ta	Tantalum	45.1	0.93
74	W	Tungsten	23.3	0.83
14	Si	Silicon	17.3	0.99
22	Ti	Titanium	6.9	0.98
28	Ni	Nickel	2.7	0.91
42	Mo	Molybdenum	1.8	0.89
6	C	Carbon	1.3	0.74
12	Mg	Magnesium	1	0.95
24	Cr	Chromium	0.6	0.82
27	Co	Cobalt	0	1

Spot 2 is a coarsen primary gamma prime precipitate. This is because the grain size has elongated and formed an awkward shape. From the spectrum in Figure 13, it shows that the highest peak is Nickel. This justify that the phase at spot 2 is gamma prime precipitate. Table 5 shows the other elements that presence at that spot.

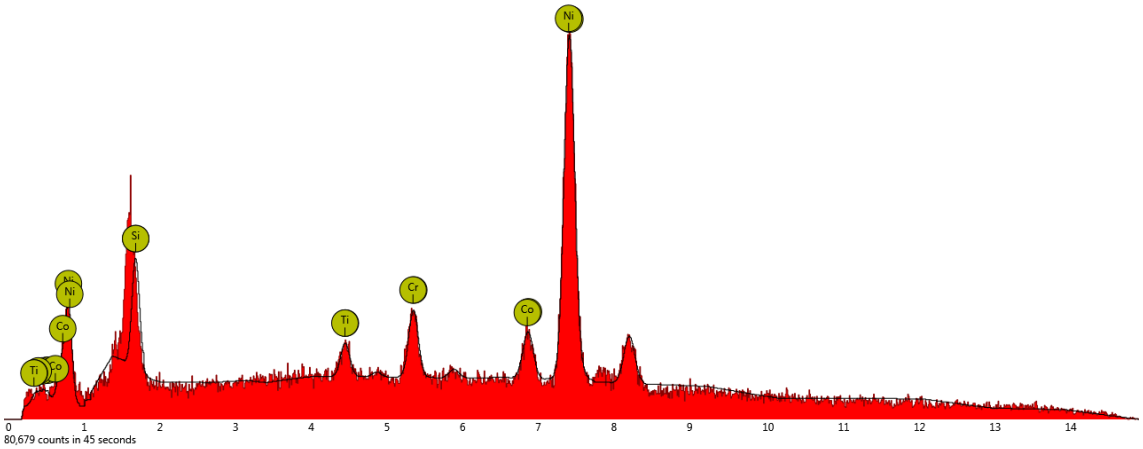

Figure 13: Elemental composition at spot 2, location A3

Table 5: Elements detected at spot 2, location A3

Atomic Number	Element Symbol	Element Name	Concentration (%)	Certainty
28	Ni	Nickel	79.2	0.99
27	Co	Cobalt	8.4	0.95
24	Cr	Chromium	5.6	0.96
14	Si	Silicon	4.9	0.97
22	Ti	Titanium	2	0.93

Meanwhile at spot 3 is the primary gamma prime precipitate. The distribution of the precipitates is bimodal fine primary gamma prime precipitates are mixed around with coarsen-elongated primary gamma prime precipitate. Figure 14 also shows the spectrum with Nickel being the highest peak thus dominates the concentration percentage, which justify that the phases at spot 3 is gamma prime precipitate. Table 5 shows the other elements that presence at that spot.

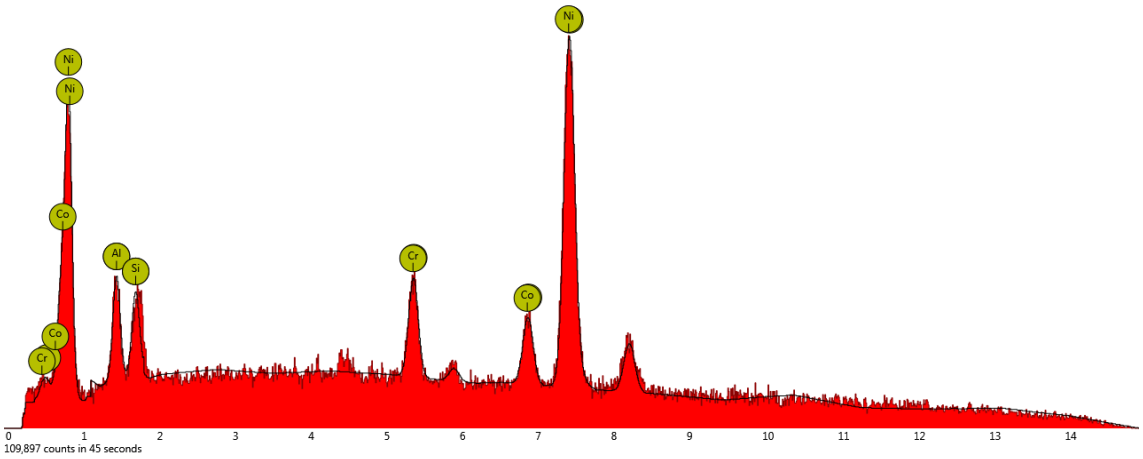

Figure 14: Elemental composition at spot 3, location A3

Table 6: Elements detected at spot 3, location A3

Atomic Number	Element Symbol	Element Name	Concentration (%)	Certainty
28	Ni	Nickel	73	0.99
27	Co	Cobalt	10.9	0.96
24	Cr	Chromium	7.4	0.97
13	Al	Aluminium	5.3	0.97
14	Si	Silicon	3.4	0.96

Spot 4 was focused on the very tiny and discrete grains, which are the secondary gamma prime precipitate. The spectrum in Figure 15 again shows the highest peak is Nickel with no Carbon detected. This has justified that the phases at spot 2 is secondary gamma prime precipitate, considering the tiny and small microstructure as well. Table 5 shows the other elements that presence at that spot.

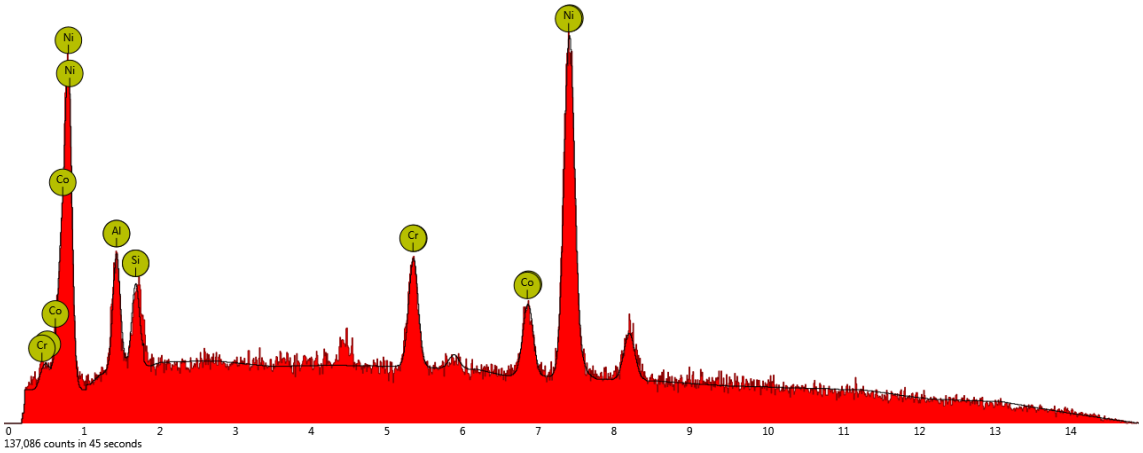

Figure 15: Elemental composition at spot 4, location A3

Table 7: Elements detected at spot 4, location A3

Atomic Number	Element Symbol	Element Name	Concentration (%)	Certainty
28	Ni	Nickel	71.2	0.99
27	Co	Cobalt	11.7	0.97
24	Cr	Chromium	8.1	0.97
13	Al	Aluminium	5.8	0.97
14	Si	Silicon	3.2	0.96

4.3.2 EDX at Location F1

Similar approach to location A3, Figure 16 shows the image obtained for analysis. Four different spots were chosen to determine its phases. Each spot would represent different phases that occurred in the microstructure. It can be observe that the distribution of gamma prime precipitate is yet again bimodal with the combination of fine primary gamma prime precipitate with elongated primary gamma prime precipitate.

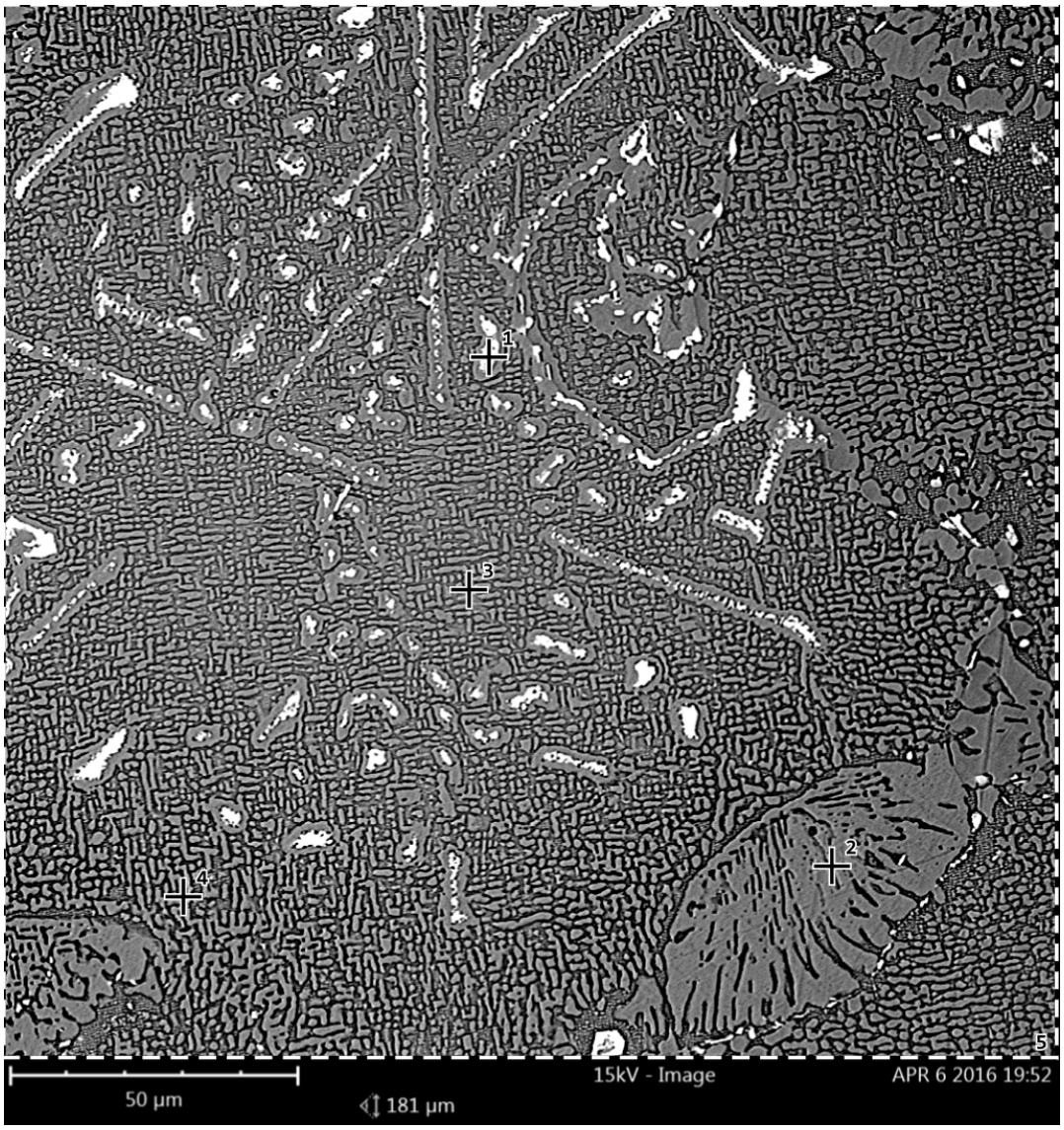

Figure 16: 4 spots taken at location F1

At spot 1 at location F1, with Tantalum and other element dominating the concentration percentage and also with the presence of Carbon, it can be justify that it is a Tantalum-based carbide. Besides that, Nickel detected at this spot is very low with only by 9.3%. This clearly proves again that the white aligned structure is carbide. Figure 17 shows that Tantalum is at the highest peak while Table 4 shows the rest of the elements present at spot 1 at this location.

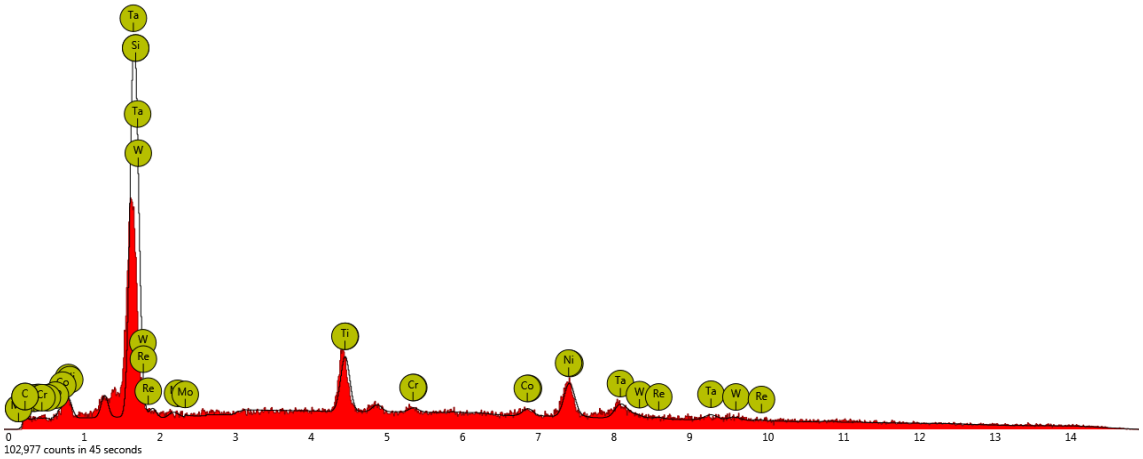

Figure 17: Elemental composition at spot 1, location F1

Table 8: Elements detected at spot 1, location F1

Atomic Number	Element Symbol	Element Name	Concentration (%)	Certainty
73	Ta	Tantalum	46.7	0.95
75	Re	Rhenium	12	0.73
74	W	Tungsten	11.9	0.8
14	Si	Silicon	10.5	0.99
28	Ni	Nickel	9.3	0.97
22	Ti	Titanium	4.7	0.98
6	C	Carbon	1.9	0.88
27	Co	Cobalt	1.6	0.91
42	Mo	Molybdenum	1	0.87
24	Cr	Chromium	0.5	0.84

Meanwhile at spot 2, a coarsen primary gamma prime precipitate is selected. It is observed that the microstructure has coarsen and thus resulting in a rougher edge of the grains. Figure 18 proves that the highest peak is Nickel while Table 5 shows the other elements that presence at that spot with Nickel recorded the concentration percentage of 74.7%.

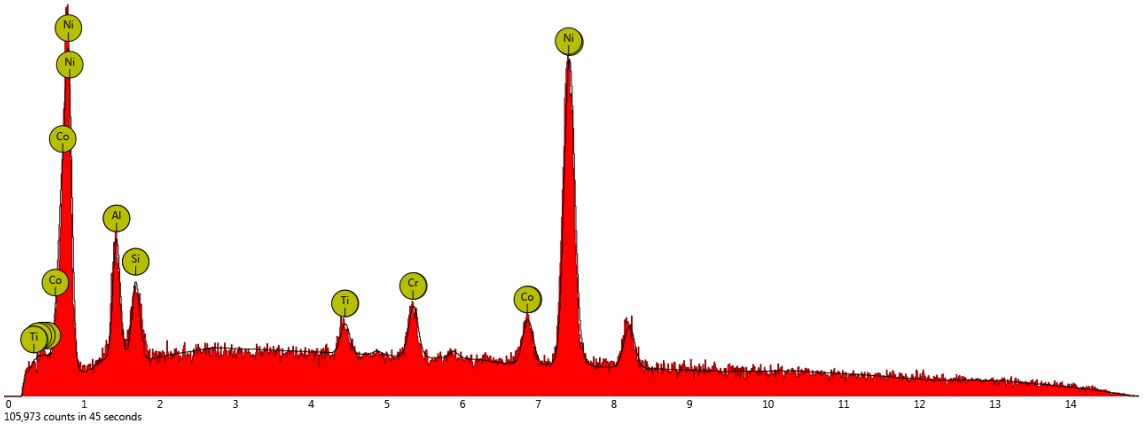

Figure 18: Elemental composition at spot 1, location A3

Table 9: Elements detected at spot 2, location F1

Atomic number	Element symbol	Element name	Concentration (%)	Certainty
28	Ni	Nickel	74.7	0.99
27	Co	Cobalt	8.5	0.96
13	Al	Aluminium	7	0.97
24	Cr	Chromium	4.4	0.96
14	Si	Silicon	3.5	0.96
22	Ti	Titanium	1.9	0.93

Spot 3 and spot 4 at location F1 are actually the same phase which is the primary gamma prime precipitate. Again, the bimodal distribution of the precipitate is observed with fine and coarsen primary gamma prime precipitates are scattered throughout the image. Figure 19 and Figure 20 show both spectrums of spot 3 and spot 4 respectively. Unsurprisingly, Nickel has recorded the highest concentration percentage at both spot. focused on the very tiny and discrete grains, which are the secondary gamma prime precipitate. The spectrum in Figure 14 again shows the highest peak is Nickel with no Carbon detected. This has justified that the phases at spot 2 is secondary gamma prime precipitate, considering the tiny and small microstructure as well. Table 5 shows the other elements that presence at that spot.

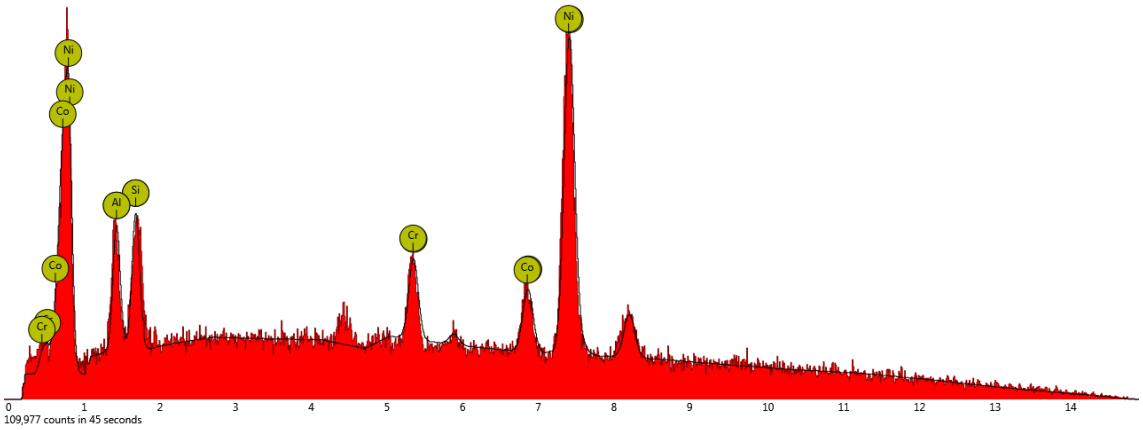

Figure 19: Elemental composition at spot 3, location F1

Table 10: Elements detected at spot 3, location F1

Atomic Number	Element Symbol	Element Name	Concentration (%)	Certainty
28	Ni	Nickel	70.6	0.99
27	Co	Cobalt	10.7	0.96
13	Al	Aluminium	6.5	0.97
24	Cr	Chromium	6.5	0.96
14	Si	Silicon	5.7	0.97

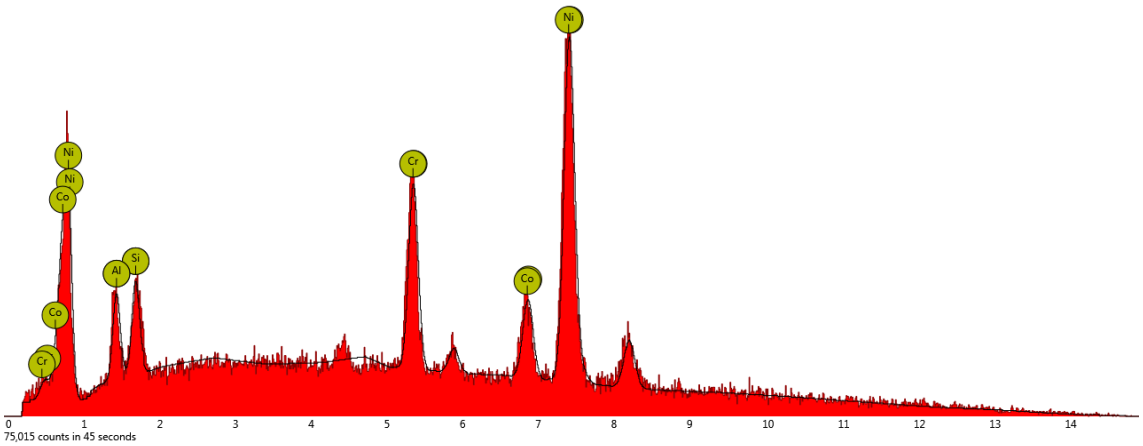

Figure 20: Elemental composition at spot 4, location F1

Table 11: Elements detected at spot 4, location F1

Atomic Number	Element Symbol	Element Name	Concentration (%)	Certainty
28	Ni	Nickel	67.6	0.99
24	Cr	Chromium	13.1	0.98
27	Co	Cobalt	12	0.96
13	Al	Aluminium	4	0.96
14	Si	Silicon	3.4	0.96

CHAPTER 5

CONCLUSION AND RECOMMENDATION

5.1 Conclusion

As for conclusion, it can be assured that the grain size of gamma prime precipitate varies at different location of the turbine blade due to different temperature that the blade was exposed during service. Each surface location of the blade was measured and the average values were compared. It can be concluded that there is significant difference when comparing the leading edge against the trailing edge and also suction surface side against the pressure surface side. Trailing edge would have a larger mean size compared to leading edge due to impingement cooling.

Other than that, from the EDX analysis as well, the results show that there are different elemental compositions appeared at a location when a number of spots were being focused on. The phases also can be determined by the shape and size variation of the gamma prime precipitate. The presence of Carbides were confirmed through EDX analysis.

This project is considered to be a successful project because the objective, which is to measure the grain size of the gamma prime precipitates of the used turbine blade and determined other phases that occurred in the microstructure are satisfied. Apart from that, the scope of study also has been fulfilled and the methodology of the project is followed accordingly. Furthermore, the results obtained as well did not contradict with the previous researches that were carried out in different studies.

5.2 Recommendation

To make a more comprehensive study relating the grain size, phases that occurred and the mechanical properties of the blade, as a recommendation, the micro hardness can be carried out. Through hardness test, the strength, creep-rupture, stress or any other mechanical properties or characteristics of the blade can be related thus the results gained will be clearer and relatable to other studies.

Other than that, to further understand about the behavior of the grain size changes, a heat treatment process can be performed as well. For the process, it is expected that the microstructure would change and the changes will be made comparisons with the current results that was obtained from this study.

REFERENCES

[1] M. P. Boyce, "Axial Flow Turbines". in *Gas Turbine Engineering Handbook* (3rd ed.). Oxford: Elsevier. 2006.

[2] R. Bowman, “Superalloys: A Primer and History,” The Minerals, Metals & Materials Society (TMS), Champion, Pennsylvania.

[3] E. Lvova and D. Nosworthy, 'Influence of Service-Induced Microstructural Changes on the Aging Kinetics of Rejuvenated Ni-Based Superalloy Gas Turbine Blades', *Journal of Materials Engineering and Performance*, vol. 10, no. 3, pp. 299-312, 2001.

[4] M. Sujata, M. Madan, K. Raghavendra, M. Venkataswamy and S. Bhaumik, “Identification of failure mechanisms in nickel base superalloy turbine blades through microstructural study,” *Engineering Failure Analysis*, no. 17, pp. 1436-1446, 2010.

[5] M. Sujata, M. Madan, K. Raghavendra, M. Venkataswamy and S. Bhaumik, “Microstructural study: an aod to determination of failure,” *Transactions of The Indian Institute of Metals*, vol. 63, no. 2-3, pp. 681-685, 2005.

[6] T. J. Carter, “Common failures in gas turbine blades”, in *Engineering Failure Analysis*, vol. 12, pp. 237-247, 2005.

[7] S. J. Donachie and M. J. Donachie, “Superalloys for High Temperature- A Primer” in *Superalloys: A Technical Guide*, 2nd ed. USA: ASM International, 2002, ch. 1, pp.6-9

[8] P. Wangyao, T. Korath, T. Harnvirojkul, V. Krongtong, W. Homkajai, “ The SEM Study of Microstructural Restoration by Reheat Treatments in Cast Superalloys Turbine Blade” in *Acta Metallurgica Slovaka,* vol. 11, pp. 25-35, 2005

[9] P. Wangyao, N. Chuankrerkkul, S. Polsilapa, P. Sopon and W. Homkrajai, “Gamma Prime Phase Stability after Long-Term Thermal Exposure in Cast Nickel Based Superalloy, IN-738”, *Chiang Mai J. Sci.* , vol. 36, no. 3, pp. 312-319, 2009.

[10] A. Lavakumar, P. K. Singh, S. Srivastava, S. Kori, L. A. Kumar, "Gamma Prime Coarsening Behavior of Nickel Super alloy Super cast 247A after Prolonged Thermal Exposures", *IOSR Journal of Mechanical and Civil Engineering (IOSR-JMCE),* pp. 37-42.

[11] S. Zhao, X. Xie, G. Smith and S. Patel, 'Gamma prime coarsening and age-hardening behaviors in a new nickel base superalloy', *Materials Letters*, vol. 58, no. 11, pp. 1784-1787, 2004.

[12] M. Doi, D. Miki, T. Moritani, T. Kozakai, "Gamma/Gamma Prime Microstructure Formed By Phase Seperation of Gamma Prime Precipitate in a Ni-Al-Ti Alloy" *Superalloys,* pp. 109-114, 2004.

[13] C. A. E. M, "New technology used in gas turbine blade materials," *Scientia et Technica Ano*, vol. XIII, no. 36, September 2007.

[14] M. Rahimian, S. Milenkovic and I. Sabirov, "Microstructure and hardness evolution in MAR-M247 Ni-based superalloy processed by controlled cooling and double heat treatment", *Journal of Alloys and Compounds*, vol. 550, pp. 339-344, 2013.

[15] H. T. Kim, S. S. Chun, X. X. Yao, Y. Fang and J. Choi, "Gamma prime (γ′) precipitating and ageing behaviours in two newly developed nickel-base superalloys", *Journal of Material Science,* no. 32, pp. 4917-4923, 1997.